Precision gaugino mass measurements as a probe of large trilinear soft terms at the ILC

Kyu Jung Bae, Howard Baer, Natsumi Nagata, and Hasan Serce

Phys. Rev. D **94**, 035015 — Published 17 August 2016

DOI: 10.1103/PhysRevD.94.035015

UT-16-23
NSF-KITP-16-083
UMN-TH-3532/16
FTPI-MINN-16/20

Precision gaugino mass measurements as a probe of large trilinear soft terms at ILC

Kyu Jung Bae[1*], Howard Baer[2,3,4†], Natsumi Nagata[4‡] and Hasan Serce[2§]

[1] *Dept. of Physics, University of Tokyo, Bunkyo-ku, Tokyo 113–0033, Japan*
[2] *Dept. of Physics and Astronomy, University of Oklahoma, Norman, OK 73019, USA*
[3] *Kavli Institute for Theoretical Physics, University of California, Santa Barbara, CA 93106 USA*
[4] *William I. Fine Theoretical Physics Institute, School of Physics and Astronomy, University of Minnesota, Minneapolis, MN 55455, USA*

Abstract

In supersymmetric models with radiatively-driven naturalness, higgsino-like electroweak-inos (EW-inos) are expected to lie in a mass range 100–300 GeV, the lighter the more natural. Such states can be pair-produced at high rates at ILC where their masses are nearly equal to the value of the superpotential μ parameter while their mass splittings depend on the gaugino masses M_1 and M_2. The gaugino masses in turn depend on trilinear soft terms—the A parameters, which are expected to lie in the multi-TeV range owing to the 125 GeV Higgs mass—via two-loop contributions to renormalization group running. We examine the extent to which ILC is sensitive to large A-terms via precision EW-ino mass measurement. Extraction of gaugino masses at the percent level or below should allow for interesting probes of large trilinear soft SUSY breaking terms under the assumption of unified gaugino masses.

[*] Email: bae@hep-th.phys.s.u-tokyo.ac.jp
[†] Email: baer@nhn.ou.edu
[‡] Email: nagat006@umn.edu
[§] Email: serce@ou.edu

1 Introduction

The initial spate of results from LHC Run 1 at $\sqrt{s} = 7$–8 TeV and Run 2 with $\sqrt{s} = 13$ TeV have been delivered and have caused a paradigm shift in expected phenomenology of supersymmetric (SUSY) models. In pre-LHC years, a rather light spectrum of sparticle masses was generally expected on the basis of naturalness: that weak-scale SUSY should not lie too far beyond the weak scale as typified by the $W,\ Z$ (and ultimately h) masses, where $m_{\rm weak} \simeq m(W, Z, h) \simeq 100$ GeV. These expectations were backed up by calculations of upper bounds on sparticle masses using the Barbieri–Giudice measure [1–5]

$$\Delta_{\rm BG} \equiv \max_i \left| \frac{\partial \log m_Z^2}{\partial \log p_i} \right| \ , \tag{1}$$

where m_Z is the Z-boson mass and the p_i label fundamental parameters of the theory, usually taken to be the unified soft SUSY breaking terms and the superpotential μ parameter. The upper bounds turned out to be typically in the range of a few hundred GeV: for instance, in Ref. [1], it was found that $m_{\tilde{g}} \lesssim 350$ GeV for $\Delta_{\rm BG} < 30$.

Naive hopes for a rapid discovery of SUSY at LHC were dashed by the reality of data wherein lately the ATLAS and CMS collaborations have produced bounds on the gluino mass of $m_{\tilde{g}} > 1.8$ TeV in simplified models assuming $\tilde{g} \to b\bar{b}\widetilde{Z}_1$ decays [6,7]. The effect of direct sparticle mass limits was compounded by the rather high value of the Higgs-boson mass $m_h \simeq 125$ GeV [8] which was discovered. Such a high Higgs mass required top squarks in the 10–100 TeV range for small stop mixing and in the few TeV range for large stop mixing. While heavy stops were allowed by the $\Delta_{\rm BG}$ measure in the focus-point region [9], they were seemingly dis-allowed by large logarithmic contributions to m_h as quantified by the high-scale large-log measure $\Delta_{\rm HS}$ [10, 11] which seemed to require *three* third generation squarks with mass $\lesssim 500$ GeV [12]. Thus, the LHC data cast a pall on overall expectations for SUSY and indeed led to doubts as to whether weak scale SUSY did actually provide nature's solution to the gauge hierarchy problem. In addition, lack of new physics at LHC cast doubt on the motivation for new accelerators such as the International Linear e^+e^- Collider (ILC) which would operate at $\sqrt{s} = 0.5$–1 TeV [13, 14]: Would there be any prospect for detection of new particles, or would the role of such a machine be mainly to tabulate assorted precision measurements as a Higgs factory? Prospects for ILC detection of any SUSY particles [15, 16] seemed dim, much less embarking on a program of precision SUSY particle measurements to determine underlying high scale Lagrangian parameters [17].

An alternative approach was to scrutinize the validity of the theoretical naturalness calculations. The most conservative approach to naturalness arises from the weak scale link between the measured value of m_Z and the fundamental SUSY Lagrangian parameters [18, 19]. Minimization of the scalar potential in the minimal supersymmetric Standard Model (MSSM) leads to the well-known relation [20]

$$\frac{m_Z^2}{2} = \frac{m_{H_d}^2 + \Sigma_d^d - (m_{H_u}^2 + \Sigma_u^u)\tan^2\beta}{\tan^2\beta - 1} - \mu^2 \tag{2}$$

$$\simeq -m_{H_u}^2 - \Sigma_u^u - \mu^2 \tag{3}$$

where Σ_u^u and Σ_d^d denote the 1-loop corrections (expressions can be found in the Appendix of Ref. [19]) to the scalar potential, $m_{H_u}^2$ and $m_{H_d}^2$ are the Higgs soft masses at the weak scale, and $\tan\beta \equiv \langle H_u\rangle/\langle H_d\rangle$ is the ratio of the Higgs vacuum expectation values (VEVs). The second line obtains for moderate to large values of $\tan\beta \gtrsim 5$ (as required by the Higgs mass calculation [21]). SUSY models requiring large cancellations between the various terms on the right-hand-side of Eq. (3) to reproduce the measured value of m_Z^2 are regarded as unnatural, or fine-tuned. In contrast, SUSY models which generate terms on the RHS of Eq. (3) which are all less than or comparable to $m_{\rm weak}$ are regarded as natural. Thus, the *electroweak* naturalness measure $\Delta_{\rm EW}$ is defined as [18, 19]

$$\Delta_{\rm EW} \equiv \max|\text{each additive term on RHS of Eq. (2)}|/(m_Z^2/2). \tag{4}$$

Including the various radiative corrections, over 40 terms contribute. Neglecting radiative corrections, and taking moderate-to-large $\tan\beta \gtrsim 5$, then $m_Z^2/2 \sim -m_{H_u}^2 - \mu^2$ so the main criterion for naturalness is that *at the weak scale*

- $m_{H_u}^2 \sim -m_Z^2$ and
- $\mu^2 \sim m_Z^2$ [22].

The value of $m_{H_d}^2$ (where $m_A \sim m_{H_d}(\text{weak})$ with m_A being the mass of the CP-odd Higgs boson) can lie in the TeV range since its contribution to the RHS of Eq. (3) is suppressed by $1/\tan^2\beta$. The largest radiative corrections typically come from the top squark sector. Requiring highly mixed TeV-scale top squarks minimizes $\Sigma_u^u(\tilde{t}_{1,2})$ whilst lifting the Higgs mass m_h to ~ 125 GeV [19]. This framework is called the radiatively-driven natural SUSY (RNS) [18, 19] scenario.

Using $\Delta_{\rm EW} < 30$ or better than 3% fine-tuning[1] then instead of earlier upper bounds, it is found that

- $m_{\tilde{g}} \lesssim 3$–4 TeV,
- $m_{\tilde{t}_1} \lesssim 3$ TeV and
- $m_{\widetilde{W}_1,\widetilde{Z}_{1,2}} \lesssim 300$ GeV.

Thus, gluinos and squarks may easily lie beyond the current reach of LHC at little cost to naturalness while only the higgsino-like lighter charginos and neutralinos are required to lie near the weak scale. The lightest higgsino $\widetilde{Z}_1$ comprises a portion of the dark matter and would escape detection at LHC. Owing to their compressed spectrum with mass gaps $m_{\widetilde{W}_1} - m_{\widetilde{Z}_1} \sim m_{\widetilde{Z}_2} - m_{\widetilde{Z}_1} \sim 10$–20 GeV, the heavier higgsinos are difficult to see at LHC owing to the rather small visible energy released from their three body decays $\widetilde{W}_1 \to f\bar{f}'\widetilde{Z}_1$ and $\widetilde{Z}_2 \to f\bar{f}\widetilde{Z}_1$ (where the f stands for SM fermions). At the ILC, on the other hand, direct searches for higgsino-like neutralinos and charginos are more promising since the ILC background is much simpler. We will briefly review ILC direct searches for neutralinos and charginos in Sec. 2.

The apparent conflict between $\Delta_{\rm EW}$ and $\Delta_{\rm BG}$ was resolved when it was pointed out that $\Delta_{\rm BG}$ was typically applied to low energy effective SUSY theories wherein the soft terms were

[1] For higher values of $\Delta_{\rm EW}$, high fine-tuning sets in and is displayed visually in Fig. 2 of Ref. [23].

introduced as independent parameters to parametrize the unknown dynamics of hidden sector SUSY breaking. If instead the soft terms are all calculable *e.g.* as multiples of the gravitino mass $m_{3/2}$ as in gravity-mediation, then positive and negative high scale contributions to m_Z^2 cancel and the measure reduces to $\Delta_{\rm EW}$ [24–26]. Likewise, if one combines all dependent contributions in the large log measure $\Delta_{\rm HS}$ then cancellations between $m_{H_u}^2(\Lambda)$ and $\delta m_{H_u}^2$ are possible so that $\Delta_{\rm HS} \simeq \Delta_{\rm EW}$: in this case the large negative correction $\delta m_{H_u}^2$ is used to drive the large GUT-scale soft term $m_{H_u}^2$ to a natural value at the weak scale.

A grand overview plot of the natural SUSY parameter space is shown in Fig. 1 where we show contours of $m_h = 123$, 125 and 127 GeV (red, green and blue contours) in the A_0 vs. m_0 plane for $\mu = 150$ GeV, $m_{1/2} = 1$ TeV, $\tan\beta = 10$ and $m_A = 2$ TeV. We also show contours of electroweak naturalness $\Delta_{\rm EW} = 30$, 100 and 400 (black, orange and brown contours). While it is possible to be highly natural for small m_0 and small A_0 (as expected in pre-LHC days), this region generates a rather light Higgs mass of typically $m_h \sim 115$–120 GeV. However, it is also possible to be highly natural if one moves to multi-TeV values of m_0 and A_0 just above the gray excluded region (where CCB=charge or color breaking minima occur). In fact, in this large m_0 and A_0 region, we also see that the Higgs mass moves up to allowed values ~ 125 GeV. Thus, the intersection of these regions—highly natural with $m_h \sim 125$ GeV—requires multi-TeV values of m_0 and A_0. In fact, in a recent paper [27], it was suggested that in models with $\mu \ll m_{\rm SUSY}$, the string landscape statistically favors as large as possible values of soft terms which are at the same time consistent with the anthropic requirement of $m_{\rm weak} \sim 100$ GeV. In this region, the EW symmetry is barely broken leading to $m_{H_u}^2({\rm weak}) \sim -m_Z^2$. Then very large, multi-TeV values of m_0 and A_0 are to be expected.

Since m_0 sets the squark and slepton mass scale, we expect if we live in this region then the matter scalars will likely be out of LHC reach. Top squarks are also likely to be beyond both LHC and ILC reach so it will be difficult to ascertain whether the trilinear terms A_0 are indeed large. However, such a large A_0 modifies the gaugino masses via two loop terms in the renormalization group evolution. If the ILC measures gaugino masses at the percent level or below, it is possible to indirectly see the large A_0 which is required for natural SUSY. In this paper, we advocate precision measurements of the lightest chargino and neutralino masses as a means to test the requirement of multi-TeV trilinear soft breaking terms.

2 Review of radiatively-driven natural SUSY at ILC

While gluino masses may range up to 4 TeV for $\Delta_{\rm EW} < 30$ [19,23,28], the 5σ reach of LHC14 for gluino pair production with ~ 1000 fb^{-1} extends only to about 2 TeV while the 95% CL exclusion for ~ 3000 fb^{-1} extends to about 2.8 TeV. Other signal channels such as same sign diboson production [29] from $pp \to \widetilde{W}_2\widetilde{Z}_4$ or $pp \to \widetilde{Z}_1\widetilde{Z}_2 j \to \ell^+\ell^- j + E_{\rm T}^{\rm miss}$ [30–32] should extend the LHC reach for natural SUSY spectrum [33].

Meanwhile, construction of the ILC would be highly propitious for natural SUSY. If natural SUSY is correct, then ILC would likely be a *higgsino factory* where the reactions $e^+e^- \to \widetilde{W}_1^+\widetilde{W}_1^-$ and $\widetilde{Z}_1\widetilde{Z}_2$ would occur at high rates provided $\sqrt{s} > 2m$(higgsino) and the semi-compressed decays would be easily visible in the clean environment of e^+e^- collisions.[2]

[2]Even in the highly compressed (but less natural) case of sub-GeV EW-ino mass gaps, precision mass

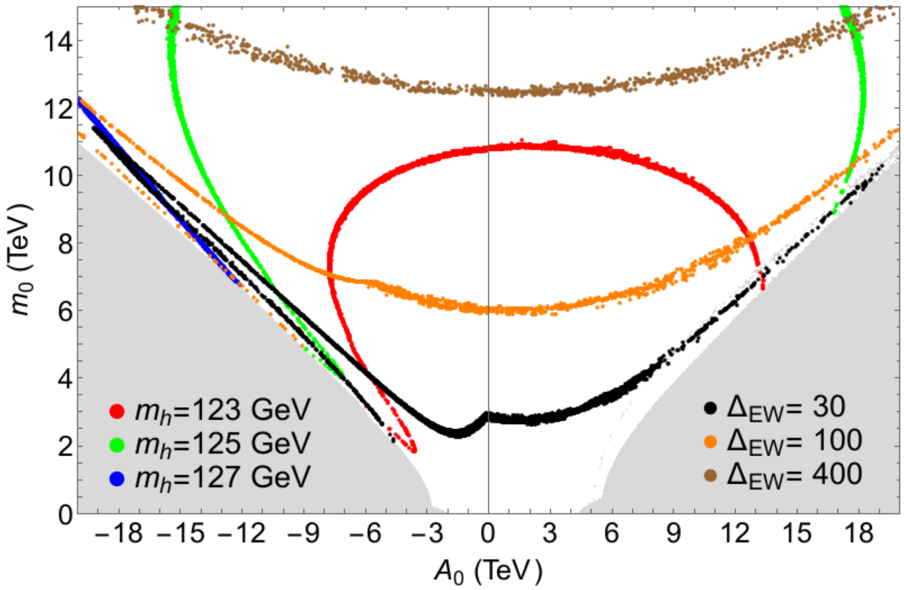

Figure 1: The A_0 vs. m_0 parameter plane for $\mu = 150$ GeV, $m_{1/2} = 1$ TeV, $\tan\beta = 10$ and $m_A = 2$ TeV. We show contours of $m_h = 123$, 125 and 127 GeV (red, green, blue). We also show contours of $\Delta_{\rm EW} = 30$, 100 and 400. The intersection of $m_h \simeq 125$ GeV and low $\Delta_{\rm EW}$ occurs along the edges of the allowed region at very large values of A_0.

A detailed phenomenological study of ILC measurements for RNS has been presented in Ref. [35]. More detailed studies are in progress using realistic detector simulations and more thorough background generation [36]. Briefly, the reaction $e^+e^- \to \widetilde{W}_1^+\widetilde{W}_1^-$ followed by one $\widetilde{W}_1 \to \ell\nu_\ell\widetilde{Z}_1$ and the other $\widetilde{W}_1 \to q\bar{q}'\widetilde{Z}_1$ will allow for the $m_{\widetilde{W}_1} - m_{\widetilde{Z}_1}$ mass gap extraction to sub-percent level via measurement of the dijet invariant mass. In addition, measurement of the kinematic lower and upper endpoints of the dijet energy $E(jj)$ distribution will allow for precision determination of $m_{\widetilde{W}_1}$ and $m_{\widetilde{Z}_1}$ [15, 16, 35]. Typically these endpoint measurements are expected to yield EW-ino masses at the percent level at ILC. In addition, using the variable beam polarization and the variable beam energy—for instance to do threshold scans—should allow per mille precision on extracting these mass values [13].

Likewise, the reaction $e^+e^- \to \widetilde{Z}_1\widetilde{Z}_2$ followed by $\widetilde{Z}_2 \to \ell^+\ell^-\widetilde{Z}_1$ will allow the $m_{\widetilde{Z}_2} - m_{\widetilde{Z}_1}$ mass gap to be extracted at sub percent precision from the $m(\ell^+\ell^-)$ upper bound. The endpoints of the $E(\ell^+\ell^-)$ distribution should allow extraction of $m_{\widetilde{Z}_2}$ and $m_{\widetilde{Z}_1}$ to percent or better precision. Threshold scans are again possible which could reach per mille precision on $m_{\widetilde{Z}_2}$ and $m_{\widetilde{Z}_1}$.

While the values of $m_{\widetilde{W}_1}$, $m_{\widetilde{Z}_2}$ and $m_{\widetilde{Z}_1}$ are all expected to be $\sim \mu$, the mass gaps will depend on the bino and wino contamination of the mainly-higgsino eigenstates. By combining precision mass measurements of $m_{\widetilde{Z}_{1,2}}$ and $m_{\widetilde{W}_1}$ with production cross sections (at 3% level) and measurements of Higgs decay properties [37–40] (which help constrain $\tan\beta$), then it has been shown in the case of two benchmark studies [36] that the weak scale bino M_1 and wino

measurements are possible by using initial state photon radiation [34].

M_2 masses can be extracted to high precision. Using the Fittino program [41] to fit the 10 weak scale pMSSM10 parameters to the above measurements, the gaugino masses could be extracted to $\sim 5-10\%$ level [42] and $\tan\beta$ can be determined (by including as well precision Higgs measurements) to $\sim 10 \pm 2$ for the particular benchmarks which have been studied.

However, much more can be done. The exact level of precision which is reached will be dependent on the ILC run plan and whether run time is devoted to continuum versus threshold scans. These virtual gaugino mass extractions will only be aided if further measurements of $\tan\beta$ can be gained in the case where the heavy Higgs bosons H or A are accessible to LHC (or later at $\sqrt{s} = 1$ TeV ILC) searches. In addition, other EW-ino reactions such as $e^+e^- \to \widetilde{Z}_{1,2}\widetilde{Z}_3$ may ultimately be accessible which would involve direct production of the mainly bino $\widetilde{Z}_3$ state. At even higher energies, it may be possible to directly produce the mainly wino states $\widetilde{Z}_4$ and $\widetilde{W}_2$ via $e^+e^- \to \widetilde{Z}_{1,2}\widetilde{Z}_4$ or $\widetilde{W}_1^{\pm}\widetilde{W}_2^{\mp}$. What is likely is that– for SUSY with radiatively-driven naturalness and light higgsinos– are very rich program of assorted SUSY measurements awaits the ILC program where the level of precision measurements is mainly limited by the various lucrative run-plan options.

3 Testing multi-TeV trilinears via determination of gaugino masses

In this section, we present large A-term effects on gaugino masses via the renormalization group evolution from the high energy scale to the weak scale. The two-loop renormalization group equations (RGEs) for the U(1), SU(2)$_L$ and SU(3)$_C$ gaugino masses in the $\overline{\rm DR}$ scheme read [43] :

$$\frac{dM_1}{dt} = \frac{2}{16\pi^2}\frac{33}{5}g_1^2 M_1 + \frac{2g_1^2}{(16\pi^2)^2}\left[\frac{199}{25}g_1^2(2M_1) + \frac{27}{5}g_2^2(M_1+M_2) + \frac{88}{5}g_3^2(M_1+M_3) + \frac{26}{5}f_t^2(A_t - M_1) + \frac{14}{5}f_b^2(A_b - M_1) + \frac{18}{5}f_\tau^2(A_\tau - M_1)\right], \quad (5)$$

$$\frac{dM_2}{dt} = \frac{2}{16\pi^2}g_2^2 M_2 + \frac{2g_2^2}{(16\pi^2)^2}\left[\frac{9}{5}g_1^2(M_2+M_1) + 25g_2^2(2M_2) + 24g_3^2(M_2+M_3) + 6f_t^2(A_t - M_2) + 6f_b^2(A_b - M_2) + 2f_\tau^2(A_\tau - M_2)\right], \quad (6)$$

$$\frac{dM_3}{dt} = \frac{2}{16\pi^2}(-3)g_3^2 M_3 + \frac{2g_3^2}{(16\pi^2)^2}\left[\frac{11}{5}g_1^2(M_3+M_1) + 9g_2^2(M_3+M_2) + 14g_3^2(2M_3) + 4f_t^2(A_t - M_3) + 4f_b^2(A_b - M_3)\right], \quad (7)$$

where $t \equiv \ln Q$ with Q the renormalization scale; g_1, g_2, and g_3 are the U(1), SU(2)$_L$ and SU(3)$_C$ gauge coupling constants, respectively (we use the SU(5) normalization for g_1); f_t, f_b and f_τ are the t, b and τ Yukawa couplings, respectively.[3] While generically the one-loop contributions to

[3]The third generation neutrino Yukawa coupling f_ν also contributes to the running of M_1 and M_2 above the right-handed neutrino mass scale since in simple SO(10) based grand unified theories (GUTs) we expect $f_\nu = f_t$

dM_i/dt dominate, in the case where the soft trilinears are large, then the two loop contributions, which include the A_i terms, can make a significant effect on the M_i running [44].

In Fig. 2, we show the RG trajectories of the gaugino masses M_i versus energy scale Q starting from $Q = m_{\rm GUT}$ down to the weak scale. We work in the 2-extra-parameter non-universal Higgs model (NUHM2) [45] where matter scalars have unified masses m_0 at $Q = m_{\rm GUT}$ but where Higgs soft terms m_{H_u} and m_{H_d} are independent since they necessarily live in different GUT multiplets. For convenience, we trade the GUT scale parameters $m_{H_u}^2$ and $m_{H_d}^2$ for the weak-scale parameters μ and m_A so that the model parameter space is given by

$$m_0, m_{1/2}, A_0, \tan\beta, \mu \text{ and } m_A \quad \text{(NUHM2)}. \tag{8}$$

We use the Isajet 7.85 code for sparticle mass spectrum generation in the NUHM2 model [46]. Isajet includes complete one-loop corrections to the chargino and neutralino mass eigenstates which also contain dependence on various sparticle masses and mixings and thus on the A-parameters [47].

In Fig. 2, we adopt parameter choices $m_0 = 12$ TeV, $m_{1/2} = 0.8$ TeV, $\tan\beta = 10$, $\mu = 0.15$ TeV and $m_A = 2$ TeV. The solid lines show the M_i ($i = 1, 2, 3$) evolution for $A_0 = 0$. The dashed lines show the M_i evolution for $A_0 = -1.8m_0$. In this case, the A-terms yield a negative contribution to the right-hand-sides of Eq's (5–7) thus noticeably steepening the RG slope of the M_3 running and reducing the slopes of M_1 and M_2. The effect is especially noticeable for M_2 and M_3. Meanwhile, the dotted curves are plotted for $A_0 = +1.7m_0$. In this case, the two-loop contributions to the M_i running are positive thus steepening the slopes for M_1 and M_2 while decreasing the slope for M_3. The extraction of M_1 and M_2 to high precision, provided that the gaugino masses are unified at the GUT scale, would be an excellent measure of large A-terms although we do not directly detect scalar quarks or scalar leptons.

In Fig. 3, we show the ratios of weak-scale gaugino masses versus m_0 which are generated for $m_{1/2} = 1$ TeV, $\tan\beta = 10$, $\mu = 0.15$ TeV and $m_A = 2$ TeV but where $A_0 = -1.6m_0$, $-1.8m_0$ and $-2m_0$ (solid curves colored blue, red and green respectively) and $A_0 = +1.6m_0$, $+1.8m_0$ and $+2m_0$ (dashed curves also colored blue, red and green). The black dotted regions correspond to where 124 GeV $< m_h <$ 126 GeV. The green curves end abruptly when the parameters conspire to give CCB minima in the scalar potential. Of direct relevance to ILC is the first frame, Fig. 3(a), which shows the ratio M_2/M_1 which can be extracted from precision measurements of EW-ino masses and mixings. The ratio varies by over $\sim 3\%$ on the range shown. Given sufficient accuracy in the ILC determination of M_1 and M_2, then it should be possible to determine the *sign* of A_0 and perhaps even gain information on the magnitude of A_0.

In the event that LHC also discovers gluinos via gluino pair production, then it is possible the gluino mass can be extracted with order a few percent accuracy [48,49] (depending on event rate, dominant gluino decay modes and backgrounds). If the value of M_3 can be extracted from the gluino pole mass,[4] then also the ratios M_3/M_1 and M_3/M_2 should become relevant. These

at the GUT scale. We however ignore its effects in the following analysis—if we assume the third generation neutrino mass to be ~ 0.1 eV, the corresponding right-handed neutrino mass should be $\sim 3 \times 10^{14}$ GeV. In this case, the inclusion of the neutrino Yukawa contribution changes M_1 and M_2 by $\lesssim 0.05\%$, which is totally negligible in the present discussion.

[4]See Ref's [50, 51] for the two-loop order calculations and Ref. [52] for the leading three-loop contributions.

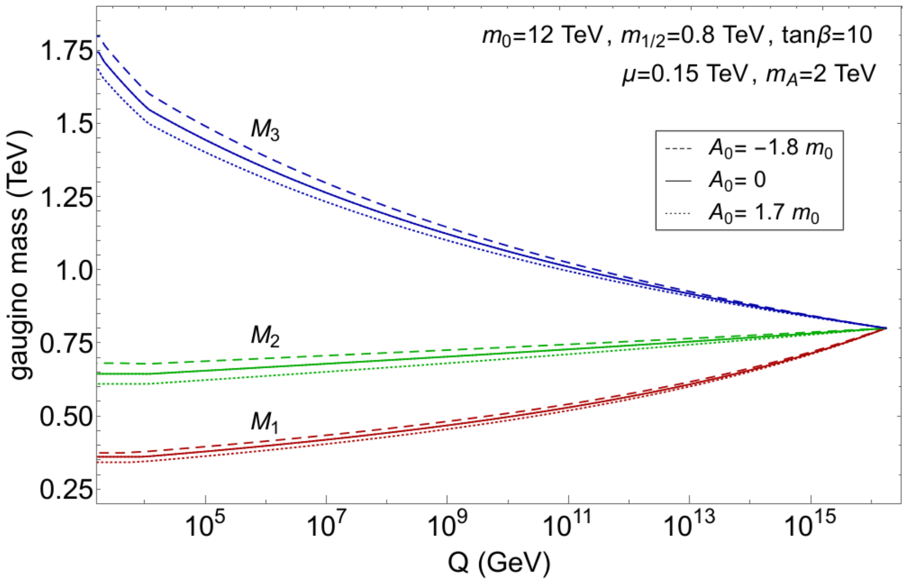

Figure 2: Evolution of gaugino masses in radiatively-driven natural SUSY for large positive and negative and small trilinear soft SUSY breaking terms.

ratios are shown versus m_0 in frames Figs. 3(b) and 3(c). The ratio M_3/M_2 especially shows a significant disparity in values depending on whether the A_0 terms are positive or negative.

In Fig. 4 we show the weak-scale gaugino mass ratios versus variation in A_0 for $m_{1/2} = 1$ TeV, $\tan\beta = 10$, $\mu = 0.15$ TeV and $m_A = 2$ TeV but where m_0 is scanned over the range $m_0 : 0 - 15$ TeV and -20 TeV $< A_0 < +20$ TeV. The gray regions are disallowed by either CCB scalar potential minima or no EWSB. The green regions yield a light Higgs mass with 124 GeV $< m_h <$ 126 GeV while the orange regions indicate $\Delta_{\rm EW} < 50$. For Fig. 4(a), we see two intersecting regions: one for positive A_0 and one for negative A_0. The low fine-tuned regions which are consistent with the measured value of m_h occur at large $|A_0|$ values indicating large mixing in the stop sector. The ratio $M_2/M_1 \gtrsim 1.81$ for the case of A_0 large negative while $M_2/M_1 \lesssim 1.81$ for A_0 large positive. We also notice that these two regions can be sufficiently separated from those which predict the correct Higgs mass but a large value of $\Delta_{\rm EW}$. In particular, $A_0 \simeq 0$ points with $m_h \simeq 125$ GeV predict $M_2/M_1 \lesssim 1.78$, which can be distinguished from the above two regions if M_2/M_1 is measured with $\sim 1\%$ accuracy. Thus, assuming unified gaugino masses, it appears precision measurements of EW-ino masses and mixings will be sensitive to details of large trilinear soft terms.

In Fig. 4(b), we show the ratio M_3/M_1 for the case where LHC14 can discover the gluino and gain an estimate of M_3. Here, we see the intersecting orange/green regions occur for $M_3/M_1 \gtrsim 4.84$ for A_0 large positive while $M_3/M_1 \sim 4.75$–4.88 for A_0 large negative. While some range of M_3/M_1 overlaps between these two cases, only the large negative A_0 accesses the smaller range $M_3/M_1 \lesssim 4.85$. In Fig. 4(c), we plot the ratio M_3/M_2 versus A_0. Here we see that large positive values of A_0 yield $M_3/M_2 \sim 2.68$–2.7 while large negative A_0 yields instead $M_3/M_2 \sim 2.62$–2.65. The two cases appear distinguishable to combined ILC and LHC precision

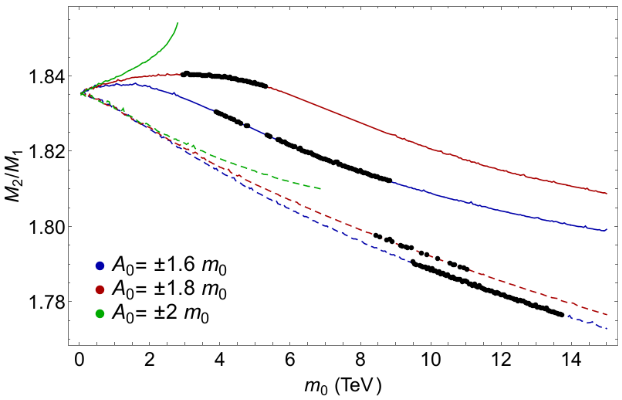

(a) M_2/M_1

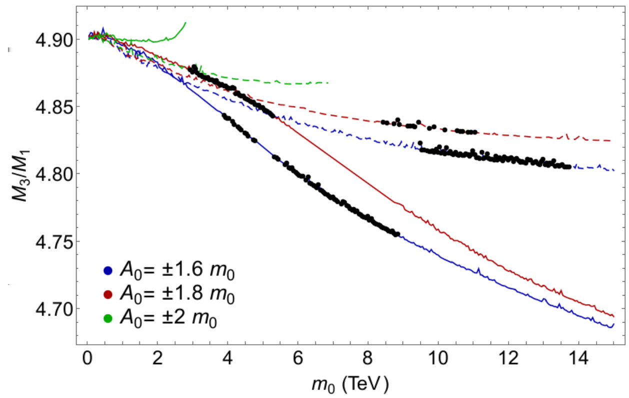

(b) M_3/M_1

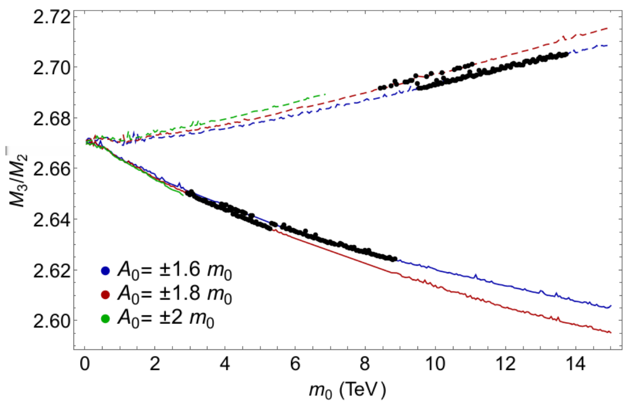

(c) M_3/M_2

Figure 3: Ratios of weak-scale gaugino masses vs. m_0 for $A_0 = \pm 1.6 m_0$, $\pm 1.8 m_0$ and $\pm 2 m_0$ for $m_{1/2} = 1$ TeV, $\tan\beta = 10$, $\mu = 150$ GeV and $m_A = 2$ TeV.

measurements.

3.1 Discussion of model dependence

Before concluding this section, we discuss some possible uncertainties in our calculations. In the calculation shown above, we assume the gaugino mass unification at the GUT scale. However, this can be spoiled by GUT-scale threshold corrections and by Planck-scale suppressed higher dimensional operators [53, 54]. These effects are expected to be $\lesssim 1\%$; however, they can be significant if the A- or B-terms for the GUT Higgs fields are much larger than gaugino masses, and/or if there are large representations of the GUT gauge group.[5]

[5] We however note that if top squarks are discovered in future collider experiments, we may infer m_0 and A_0 from the measurements of their masses, and in this case precision gaugino mass measurements in turn allow us to extract the soft parameters for the GUT Higgs fields via the GUT threshold corrections, just like the precise determination of the gauge couplings enables us to extract the mass spectrum of the GUT-scale fields via the GUT threshold corrections to the gauge couplings [55]. In this sense, precision gaugino mass measurements are of importance even if the A-terms are directly measured.

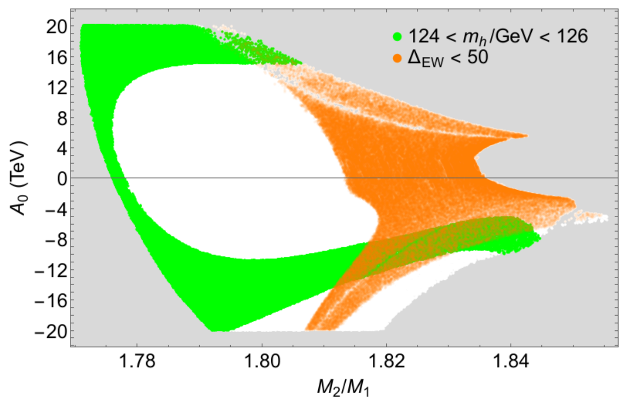

(a) M_2/M_1

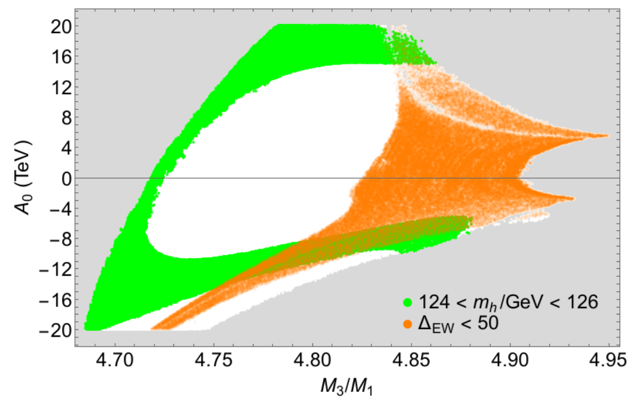

(b) M_3/M_1

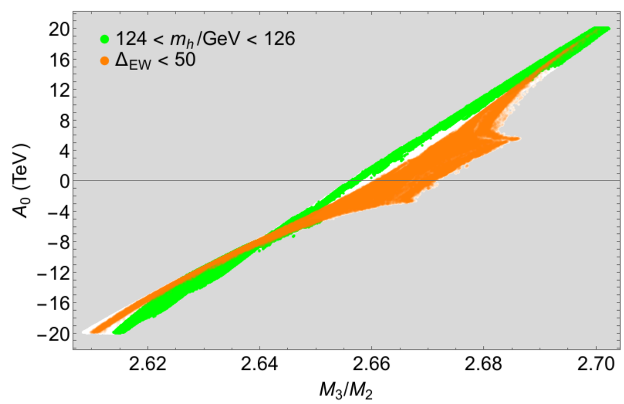

(c) M_3/M_2

Figure 4: Ratios of weak scale gaugino masses vs. A_0 for $m_{1/2} = 1$ TeV, $\tan\beta = 10$, $\mu = 150$ GeV and $m_A = 2$ TeV but with m_0 scanned over the range 0–15 TeV and -20 TeV $< A_0 < +20$ TeV.

In the event that gaugino masses are not unified, then extrapolation of the measured values of M_1 and M_2 to high scales will intersect at some point other than $Q = m_{\rm GUT}$ where the gauge couplings unify. This situation is illustrated in Fig. 5 where in frame (a) we show the running of gauge couplings while in frame (b) we show the running of gaugino masses from the compactified M-theory model of Ref. [56]. If such a theory were discovered, then the precision measurements of M_1 and M_2 at LHC and/or ILC would be extrapolated in energy to meet at a unification point other than the energy scale where the gauge couplings unify. If M_3 is also measured, then the non-unification of all three gaugino masses would be apparent.

Precision gaugino mass measurements also play an important role in testing the split-SUSY type mass spectrum [57], where soft masses are taken to be $\mathcal{O}$(100–1000) TeV and gaugino masses and A-terms are suppressed by loop factors, with which the 125 GeV Higgs mass can be obtained [58]. In this case, gaugino masses are induced via anomaly mediation and proportional to the corresponding gauge coupling beta functions [59], which results in different gaugino mass ratios from those in the unified gaugino mass case. Deviations from the anomaly-mediation

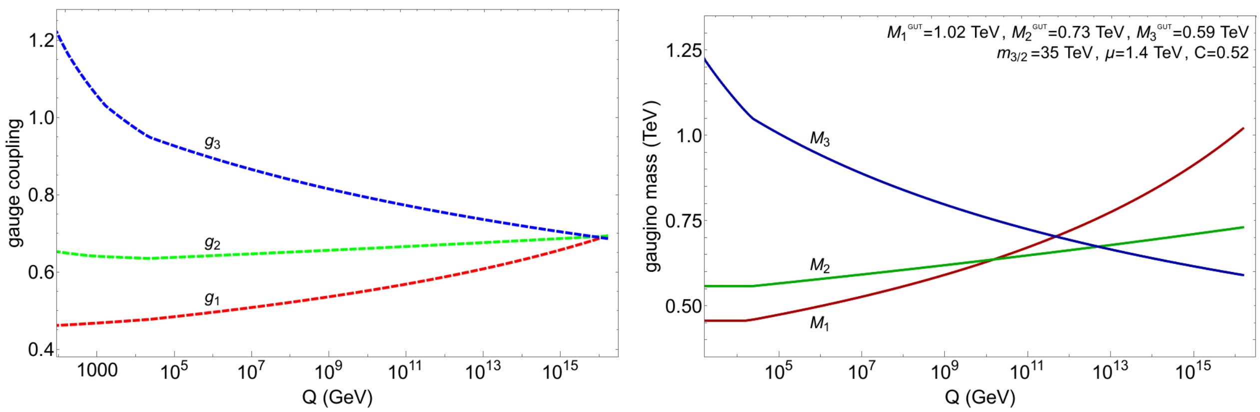

(a) gauge coupling running (b) gaugino mass running

Figure 5: In (a), we show the running of gauge couplings and in (b) we show running of gaugino masses in the G2MSSM model of Ref. [56] with $m_0 = 24.2$ TeV, $A_0 = 25.2$ TeV (or $m_{3/2} = 35$ TeV, $C = 0.52$), $\tan\beta = 8$, $\mu = 1.4$ TeV and $M_1(m_{\rm GUT}) = 1.02$ TeV, $M_2(m_{\rm GUT}) = 0.73$ TeV and $M_3(m_{\rm GUT}) = 0.59$ TeV.

relation are caused by renormalization group effects below the soft mass scale and threshold corrections by higgsino–Higgs one-loop diagrams, which enable us to extract information on the SUSY scale and higgsino/heavy Higgs mass spectrum through gaugino mass measurements.

Some discussion concerns whether the correct theory of the world around the TeV is the MSSM or some larger construct such as the NMSSM [60]. In the example of the NMSSM, a gauge singlet superfield $\hat{S}$ is added to the theory with coupling $\hat{f}_{\rm NMSSM} \ni \lambda\hat{S}\hat{H}_u\hat{H}_d$ with motivation to generate the superpotential μ-term dynamically via a VEV of S (labelled as s) and where then $\mu_{\rm eff} = \lambda s$. The theory then contains additional neutral scalar and pseudoscalar physical Higgs states along with a spin-1/2 singlino $\tilde{s}$ which mixes with the usual four neutralinos. For naturalness, $\mu_{\rm eff} \sim m_Z$ is required. The $s \sim m_Z$ case induces strong mixing between singlet and MSSM Higgs fields, which is disfavored by the current Higgs data. If $s \gg m_Z$, then the singlino decouples and thus the EW-ino sector resembles the MSSM one, and the present result is also applicable to this case. The precision Higgs coupling measurements at the ILC, determined to an accuracy of $\sim 1\%$ [61], lead us to examine the Higgs-singlet mixing which is related to the size of λ. The direct production of higgsinos, on the other hand, determines $\mu_{\rm eff}$, and possibly the size of the VEV s once the value of λ is extracted from Higgs precision measurements. This enables us to predict the singlino-higgsino mixing, and this prediction can be tested by precision measurements of the other neutralino states. Such an interplay between the direct neutralino measurements and indirect Higgs coupling measurements can only be done at lepton colliders such as the ILC. Clearly, a detailed study of precision EW-ino measurements on distinguishing between MSSM and NMSSM would be warranted, but is beyond the scope of the present study.

4 An example case study

In this section, we present an example case study to see how well a suite of precision EW-ino/Higgs boson mass and coupling measurements at ILC can distinguish the magnitude and sign of the soft trilinear A_0 parameter. We will assume an NUHM2 benchmark point with parameters $m_0 = 5$ TeV, $m_{1/2} = 1$ TeV, $A_0 = -8.3$ TeV, $\tan\beta = 10$, $\mu = 150$ GeV and $m_A = 2$ TeV. Initially, we assume the following ILC precision measurements:

- physical masses of EW-inos $\widetilde{Z}_2$, $\widetilde{Z}_1$ and $\widetilde{W}_1$ to 1% (later, to ± 0.4 GeV),
- cross section times branching fraction for $e^+e^- \to \widetilde{W}_1^+\widetilde{W}_1^- \to (\ell\nu_\ell\widetilde{Z}_1) + (q\bar{Q}\widetilde{Z}_1)$ and $e^+e^- \to \widetilde{Z}_1\widetilde{Z}_2 \to \ell^+\ell^-\widetilde{Z}_1\widetilde{Z}_1$ to 3%,
- Higgs mass m_h to ± 1 GeV (the physical measurement can take place at ILC to $\sim \pm 30$ MeV but we assume a theory error of $\sim 1\%$ on the m_h calculation),
- Higgs couplings $\kappa_b, \kappa_t, \kappa_\tau, \kappa_W, \kappa_Z, \kappa_g, \kappa_\gamma$ to precision levels given in Fig. 5 of Ref. [61].

Assuming the above measurement uncertainties, we will next scan over NUHM2 parameter space values

- $m_0 : 1 - 10$ TeV,
- $m_{1/2} : 0.5 - 2$ TeV,
- $A_0 : -2m_0 \to +2m_0$,
- $\tan\beta : 5 - 50$,
- $\mu : 140 - 160$ GeV,
- $m_A : 0.5 - 5$ TeV.

We will accept points which generate mass/coupling values which lie within the above "measured" ranges and plot them in the M_2/M_1 vs. A_0 plane.

From Fig. 6(a), we see that 1% precision on the physical (Higgsino-like) EW-ino mass measurements (shown by purple points) is not good enough to determine the weak scale gaugino masses also at the percent level, and so it is hard to distinguish the sign of A_0. In part this is due to $\tan\beta$ not being well-enough determined such as to extract the weak scale Lagrangian gaugino masses to sufficient precision. If additional background suppression is found, or if much greater integrated luminosity is obtained, or if threshold scans are made, then it is possible to reach EW-ino mass measurements in the per mille range [14]. In frame 6(b), we plot the locus of scan points consistent with the above suite of ILC measurements, but this time squeezing the error bar on the EW-ino pole masses to ± 0.4 GeV. For this precision or greater, then the top branch disappears and the measured values would select out the branch with a large negative A_0 term.

An additional discrimination may come if the ILC undergoes an energy upgrade to $\sqrt{s} \sim 1$ TeV. In this case, then the bino-like and wino-like states can become directly accessible via

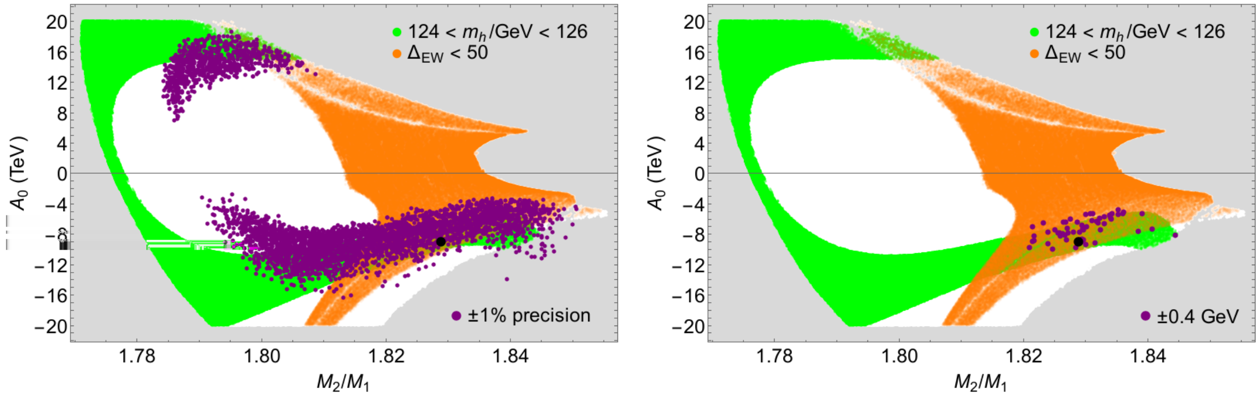

(a) EW-inos to ±1%

(b) EW-inos to ±0.4 GeV

Figure 6: Locus of benchmark point (black) and scan points (purple) which are consistent with the suite of ILC precision EW-ino and Higgs measurements as stated in text.

e.g. $e^+e^- \to \widetilde{Z}_2\widetilde{Z}_3$, $e^+e^- \to \widetilde{W}_1\widetilde{W}_2$ or $\widetilde{Z}_2\widetilde{Z}_4$ production [35]. Measurement of the bino-like $\widetilde{Z}_3$ and/or the wino-like $\widetilde{Z}_4$ and $\widetilde{W}_2$ states would provide additional discrimination. We plot the locus of scan points from the above suite of measurements (with 1% mass precision) in Fig. 7 in the $m_{\widetilde{Z}_3}$ vs. $m_{\widetilde{W}_2}$ mass plane. Blue dots denote $A_0 < 0$ while red dots denote $A_0 > 0$. Given sufficient precision in extracting the gaugino-like EW-ino states, then one ought to lie predominantly on the blue or red band. This provides an additional or alternative check at least on the sign of A_0.

5 Conclusions

In the post LHC8 world with an improved understanding of electroweak naturalness in SUSY models, then we are directed to expect the existence of rather light higgsino-like $\widetilde{W}_1^\pm$ and $\widetilde{Z}_{1,2}$ with mass $\sim 100-250$ GeV, the closer to m_h the better. Such light EW-inos are difficult to see at LHC (due to only soft tracks emerging from their decays) but should be easily visible in the clean environment of an e^+e^- collider such as ILC with $\sqrt{s} \gtrsim 2m(\text{higgsino})$. While it is expected that $m_{\widetilde{W}_1,\widetilde{Z}_{1,2}} \sim |\mu|$, the mass splittings $m_{\widetilde{W}_1} - m_{\widetilde{Z}_1}$ and $m_{\widetilde{Z}_2} - m_{\widetilde{Z}_1}$ are sensitive to the gaugino masses M_1 and M_2 via mixing effects.

From the rather high value of m_h, we also expect large trilinear soft terms A_t which contribute to large mixing in the stop sector and an uplifting of m_h. One way to test the presence of large trilinear soft terms is to look for their influence on the gaugino mass running which occurs at two-loop level. We point out that the sign of A_0 and its magnitude influence the expected ratios of gaugino masses which may be measured at ILC. From our results shown in Fig's 3 and 4, we would expect gaugino mass extraction at the $\sim 1\%$ level or below to allow for tests of large trilinear soft terms. Such measurements would likely push the experimental capabilities to their limits, and would motivate a program which includes direct threshold measurements of $\widetilde{W}_1^\pm\widetilde{W}_1^\mp$ and $\widetilde{Z}_1\widetilde{Z}_2$ production. If these are supplemented with measurements of direct bino

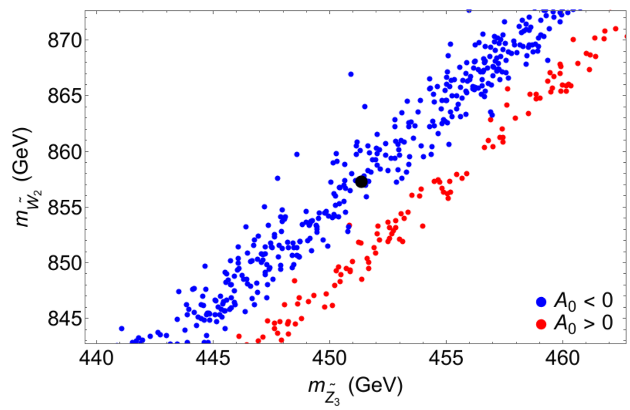

Figure 7: Locus of benchmark point (black) and scan points (red for $A_0 > 0$ and blue for $A_0 < 0$) which are consistent with the suite of ILC precision EW-ino and Higgs measurements as stated in text.

or wino production, via *e.g.* $\widetilde{Z}_{1,2}\widetilde{Z}_3$ and $\widetilde{W}_1^{\pm}\widetilde{W}_2^{\mp}$ production, then so much the better. Thus, this work motivates a dedicated program of precision measurements of EW-ino properties at a machine such as ILC which may test Lagrangian parameters well-removed from just those that directly determine the EW-ino masses.

Acknowledgments

This work was supported in part by the US Department of Energy, Office of High Energy Physics and in part by the National Science Foundation under Grant No. NSF PHY11-25915. KJB is supported by Grant-in-Aid for Scientific research No. 26104009. The work of NN is supported by the DOE grant DE-SC0011842 at the University of Minnesota. HB would like to thank the William I. Fine Institute for Theoretical Physics (FTPI) at the University of Minnesota for hospitality while this work was initiated and KITP Santa Barbara where this work was completed. The computing for this project was performed at the OU Supercomputing Center for Education & Research (OSCER) at the University of Oklahoma (OU).

References

[1] R. Barbieri and G. F. Giudice, Nucl. Phys. B **306** (1988) 63.

[2] S. Dimopoulos and G. F. Giudice, Phys. Lett. B **357** (1995) 573.

[3] G. W. Anderson and D. J. Castano, Phys. Lett. B **347** (1995) 300; G. W. Anderson and D. J. Castano, Phys. Rev. D **52** (1995) 1693; G. W. Anderson and D. J. Castano, Phys. Rev. D **53** (1996) 2403.

[4] P. H. Chankowski, J. R. Ellis and S. Pokorski, Phys. Lett. B **423** (1998) 327; P. H. Chankowski, J. R. Ellis, M. Olechowski and S. Pokorski, Nucl. Phys. B **544** (1999) 39.

[5] S. Cassel, D. M. Ghilencea and G. G. Ross, Phys. Lett. B **687** (2010) 214; S. Cassel, D. M. Ghilencea, S. Kraml, A. Lessa and G. G. Ross, JHEP **1105** (2011) 120.

[6] The ATLAS collaboration, ATLAS-CONF-2015-067.

[7] V. Khachatryan *et al.* [CMS Collaboration], [arXiv:1602.06581 [hep-ex]].

[8] G. Aad *et al.* [ATLAS and CMS Collaborations], Phys. Rev. Lett. **114**, 191803 (2015).

[9] J. L. Feng, K. T. Matchev and T. Moroi, Phys. Rev. D **61** (2000) 075005; J. L. Feng, K. T. Matchev and T. Moroi, hep-ph/0003138; J. L. Feng and D. Sanford, Phys. Rev. D **86** (2012) 055015.

[10] R. Harnik, G. D. Kribs, D. T. Larson and H. Murayama, Phys. Rev. D **70** (2004) 015002.

[11] R. Kitano and Y. Nomura, Phys. Rev. D **73**, 095004 (2006).

[12] M. Papucci, J. T. Ruderman and A. Weiler, JHEP **1209** (2012) 035.

[13] H. Baer *et al.*, arXiv:1306.6352 [hep-ph].

[14] G. Moortgat-Pick *et al.*, Eur. Phys. J. C **75** (2015) no.8, 371.

[15] T. Tsukamoto, K. Fujii, H. Murayama, M. Yamaguchi and Y. Okada, Phys. Rev. D **51** (1995) 3153.

[16] H. Baer, R. B. Munroe and X. Tata, Phys. Rev. D **54** (1996) 6735.

[17] G. A. Blair, W. Porod and P. M. Zerwas, Phys. Rev. D **63** (2001) 017703; G. A. Blair, W. Porod and P. M. Zerwas, Eur. Phys. J. C **27** (2003) 263.

[18] H. Baer, V. Barger, P. Huang, A. Mustafayev and X. Tata, Phys. Rev. Lett. **109** (2012) 161802.

[19] H. Baer, V. Barger, P. Huang, D. Mickelson, A. Mustafayev and X. Tata, Phys. Rev. D **87** (2013) 115028.

[20] H. Baer and X. Tata, *Weak Scale Supersymmetry: From Superfields to Scattering Events*, (Cambridge University Press, 2006).

[21] M. Carena and H. E. Haber, Prog. Part. Nucl. Phys. **50** (2003) 63.

[22] K. L. Chan, U. Chattopadhyay and P. Nath, Phys. Rev. D **58** (1998) 096004; S. Akula, M. Liu, P. Nath and G. Peim, Phys. Lett. B **709** (2012) 192; M. Liu and P. Nath, Phys. Rev. D **87** (2013) 9, 095012.

[23] H. Baer, V. Barger and M. Savoy, Phys. Rev. D **93** (2016), 035016.

[24] H. Baer, V. Barger and D. Mickelson, Phys. Rev. D **88** (2013) 095013.

[25] H. Baer, V. Barger, D. Mickelson and M. Padeffke-Kirkland, Phys. Rev. D **89** (2014) 115019.

[26] A. Mustafayev and X. Tata, Indian J. Phys. **88** (2014) 991; X. Tata, Phys. Scripta **90** (2015) 108001.

[27] H. Baer, V. Barger, M. Savoy and H. Serce, arXiv:1602.07697 [hep-ph].

[28] H. Baer, V. Barger and M. Savoy, Phys. Rev. D **93** (2016), 075001.

[29] H. Baer, V. Barger, P. Huang, D. Mickelson, A. Mustafayev, W. Sreethawong and X. Tata, Phys. Rev. Lett. **110** (2013), 151801; H. Baer, V. Barger, P. Huang, D. Mickelson, A. Mustafayev, W. Sreethawong and X. Tata, JHEP **1312** (2013) 013.

[30] Z. Han, G. D. Kribs, A. Martin and A. Menon, Phys. Rev. D **89** (2014), 075007.

[31] H. Baer, A. Mustafayev and X. Tata, Phys. Rev. D **90** (2014), 115007.

[32] C. Han, D. Kim, S. Munir and M. Park, JHEP **1504** (2015) 132.

[33] H. Baer, V. Barger, M. Savoy and X. Tata, arXiv:1604.07438 [hep-ph].

[34] C. H. Chen, M. Drees and J. F. Gunion, Phys. Rev. Lett. **76** (1996) 2002; M. Berggren, F. Brmmer, J. List, G. Moortgat-Pick, T. Robens, K. Rolbiecki and H. Sert, Eur. Phys. J. C **73** (2013), 2660.

[35] H. Baer, V. Barger, D. Mickelson, A. Mustafayev and X. Tata, JHEP **1406** (2014) 172.

[36] See *e.g.* talk by J. Yan at European Linear Collider Workshop, Santander, Spain, May 30-June 5, 2016; J. Yan, S.-L. Lehtinen, J. List, M. Bergren, K. Fujii, T. Tanabe and H. Baer, work in preparation.

[37] T. Han, Z. Liu and J. Sayre, Phys. Rev. D **89** (2014) 113006; M. E. Peskin, arXiv:1312.4974 [hep-ph]; S. Dawson, A. Gritsan, H. Logan, J. Qian, C. Tully, R. Van Kooten, A. Ajaib and A. Anastassov *et al.*, arXiv:1310.8361 [hep-ex].

[38] M. Endo, T. Moroi and M. M. Nojiri, JHEP **1504**, 176 (2015).

[39] K. J. Bae, H. Baer, N. Nagata and H. Serce, Phys. Rev. D **92** (2015), 035006.

[40] M. Kakizaki, S. Kanemura, M. Kikuchi, T. Matsui and H. Yokoya, Int. J. Mod. Phys. A **30**, no. 33, 1550192 (2015).

[41] P. Bechtle, K. Desch and P. Wienemann, Comput. Phys. Commun. **174** (2006) 47.

[42] Talk by S.-L. Lehtinen at SUSY 2016 meeting, Melbourne, AU, July 6, 2016.

[43] S. P. Martin and M. T. Vaughn, Phys. Lett. B **318**, 331 (1993); Y. Yamada, Phys. Rev. Lett. **72**, 25 (1994); S. P. Martin and M. T. Vaughn, Phys. Rev. D **50** (1994) 2282.

[44] H. Baer, S. Kraml, A. Lessa, S. Sekmen and H. Summy, Phys. Lett. B **685** (2010) 72.

[45] D. Matalliotakis and H. P. Nilles, Nucl. Phys. B **435** (1995) 115; P. Nath and R. L. Arnowitt, Phys. Rev. D **56** (1997) 2820; J. Ellis, K. Olive and Y. Santoso, Phys. Lett. **B539** (2002) 107; J. Ellis, T. Falk, K. Olive and Y. Santoso, Nucl. Phys. **B652** (2003) 259; H. Baer, A. Mustafayev, S. Profumo, A. Belyaev and X. Tata, JHEP**0507** (2005) 065.

[46] ISAJET, by H. Baer, F. Paige, S. Protopopescu and X. Tata, hep-ph/0312045.

[47] D. Pierce and A. Papadopoulos, Phys. Rev. D **50** (1994) 565; D. Pierce and A. Papadopoulos, Nucl. Phys. B **430** (1994) 278; A. B. Lahanas, K. Tamvakis and N. D. Tracas, Phys. Lett. B **324** (1994) 387; M. Drees, M. M. Nojiri, D. P. Roy and Y. Yamada, Phys. Rev. D **56** (1997) 276 Erratum: [Phys. Rev. D **64** (2001) 039901]; D. M. Pierce, J. A. Bagger, K. T. Matchev and R. j. Zhang, Nucl. Phys. B **491** (1997) 3.

[48] H. Baer, V. Barger, G. Shaughnessy, H. Summy and L. t. Wang, Phys. Rev. D **75** (2007) 095010.

[49] I. Hinchliffe, F. E. Paige, M. D. Shapiro, J. Soderqvist and W. Yao, Phys. Rev. D **55** (1997) 5520.

[50] Y. Yamada, Phys. Lett. B **623**, 104 (2005).

[51] S. P. Martin, Phys. Rev. D **72**, 096008 (2005).

[52] S. P. Martin, Phys. Rev. D **74**, 075009 (2006).

[53] J. Hisano, H. Murayama and T. Goto, Phys. Rev. D **49**, 1446 (1994).

[54] K. Tobe and J. D. Wells, Phys. Lett. B **588**, 99 (2004).

[55] J. Hisano, H. Murayama and T. Yanagida, Phys. Rev. Lett. **69**, 1014 (1992); J. Hisano, T. Kuwahara and N. Nagata, Phys. Lett. B **723**, 324 (2013).

[56] S. A. R. Ellis, G. L. Kane and B. Zheng, JHEP **1507** (2015) 081.

[57] J. D. Wells, hep-ph/0306127; N. Arkani-Hamed and S. Dimopoulos, JHEP **0506**, 073 (2005); G. F. Giudice and A. Romanino, Nucl. Phys. B **699**, 65 (2004); Erratum: [Nucl. Phys. B **706**, 487 (2005)]; N. Arkani-Hamed, S. Dimopoulos, G. F. Giudice and A. Romanino, Nucl. Phys. B **709**, 3 (2005); J. D. Wells, Phys. Rev. D **71**, 015013 (2005).

[58] G. F. Giudice and A. Strumia, Nucl. Phys. B **858**, 63 (2012); L. J. Hall and Y. Nomura, JHEP **1201**, 082 (2012); M. Ibe and T. T. Yanagida, Phys. Lett. B **709**, 374 (2012); M. Ibe, S. Matsumoto and T. T. Yanagida, Phys. Rev. D **85**, 095011 (2012); A. Arvanitaki, N. Craig, S. Dimopoulos and G. Villadoro, JHEP **1302**, 126 (2013); L. J. Hall, Y. Nomura and S. Shirai, JHEP **1301**, 036 (2013); N. Arkani-Hamed, A. Gupta, D. E. Kaplan, N. Weiner and T. Zorawski, arXiv:1212.6971 [hep-ph]; J. L. Evans, M. Ibe, K. A. Olive and T. T. Yanagida, Eur. Phys. J. C **73**, 2468 (2013); E. Bagnaschi, G. F. Giudice, P. Slavich and A. Strumia, JHEP **1409**, 092 (2014).

[59] L. Randall and R. Sundrum, Nucl. Phys. B **557**, 79 (1999); G. F. Giudice, M. A. Luty, H. Murayama and R. Rattazzi, JHEP **9812**, 027 (1998).

[60] U. Ellwanger, C. Hugonie and A. M. Teixeira, Phys. Rept. **496** (2010) 1; J. F. Gunion, Y. Jiang and S. Kraml, Phys. Lett. B **710** (2012) 454.

[61] K. Fujii *et al.*, arXiv:1506.05992 [hep-ex].